Interactions of Cytochrome *c* and Cytochrome *f* with Aspartic Acid Peptides

Shun Hirota,*,† Masaaki Endo,† Kozue Hayamizu,† Tomoya Tsukazaki,† Teruhiro Takabe,‡ Takamitsu Kohzuma,§ and Osamu Yamauchi*,†,||

Contribution from the Department of Chemistry, Graduate School of Science, and Research Center for Materials Science, Nagoya University, Chikusa-ku, Nagoya 464-8602, Japan, Research Institute, Meijo University, Tempaku-ku, Nagoya 468-8502, Japan, and Department of Chemistry, Faculty of Science, Ibaraki University, Mito, Ibaraki 310-8512, Japan

Received August 10, 1998

Abstract: Cytochrome *c* (cyt *c*) and cytochrome *f* (cyt *f*) molecular recognition characters and their structural changes due to complex formation with negatively charged aspartic acid peptides (Aspptd's) have been studied. Changes in the absorption spectrum of cyt *c* in the Soret region were detected when Aspptd's, up to *penta*-Asp, were added to the cyt *c* solution. These changes were the same as those observed when cyt *c* interacted with plastocyanin (PC), indicating that Aspptd's interacted with cyt *c* in the same way as PC. Conformational changes of cyt *c* due to interaction with Aspptd's observed by resonance Raman spectroscopy were similar to those reported for cyt *c* when bound with its native partner, cytochrome *c* oxidase. Electrochemical measurements showed that the redox potential of cyt *c* and cyt *f* shifted to lower potentials by 7−20 mV upon Aspptd binding, showing the enhancement in the electron donor ability of both cyt *c* and cyt *f* upon complex formation with Aspptd. The changes in the absorption spectrum and redox potential increased with the length and concentration of Aspptd. The observed structural and redox changes of cyt *c* and cyt *f* are attributed to adduct formations with Aspptd's by electrostatic interactions and suggest that similar changes would occur for cyt *c* and cyt *f* when interacting with proteins. Aspptd's, *tetra*- and *penta*-aspartic acid, served as competitive inhibitors of the electron transfer from cyt *c* or cyt *f* to PC, which was ascribable to the same adduct formation.

Introduction

The structure−function relationship of proteins is one the major topics of protein studies. Despite the importance of the interactions for recognition of proteins, there are only a limited number of studies on the interaction between proteins or between a protein and a peptide because the associated changes in properties are small, although it might control the protein function. We have shown that positively charged lysine peptides (Lysptd's) inhibit the electron transfer from reduced cytochrome *c* (cyt *c*) to oxidized plastocyanin (PC) and could perturb the PC structure and its redox potential.[1,2] On the other hand, Lysptd's promoted the electron transfer from $[Fe(CN)_6]^{4-}$ to oxidized plastocyanin (PC).[3] Likewise, negatively charged aspartic acid peptides (Aspptd's) could interact with cyt *c* or cytochrome *f* (cyt *f*), and actually, Aspptd's served as competitive inhibitors of electron transfer from $[Fe(CN)_6]^{4-}$ to oxidized cyt *c*.[3] Schematic views of cyt *c* and cyt *f* are depicted in Figure 1. Aspptd, which we used as a binding site model of their reaction partners, could interact with the lysine (Lys) residues at the protein surface of cyt *c* and cyt *f* and thus would affect the protein structures and their electron-transfer characters. Possible interaction sites of cyt *c* and cyt *f* for an Aspptd are shown in arrows in Figure 1.

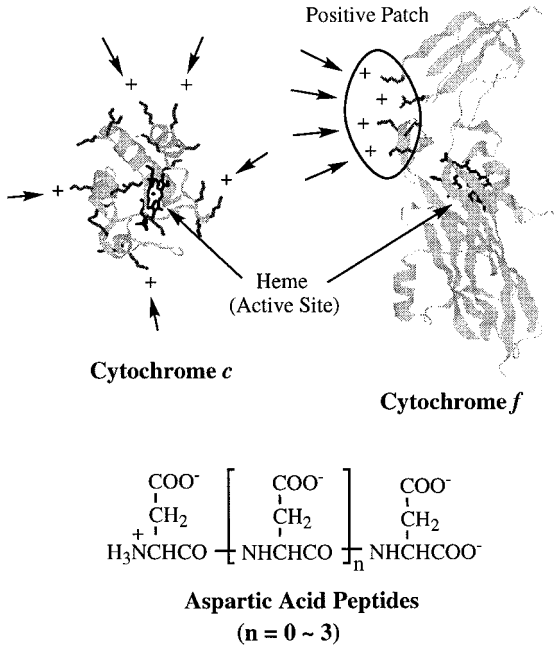

Figure 1. Schematic views of cyt *c* (horse heart) and cyt *f* (chloroplast) with aspartic acid peptides. The side chains of the lysyl residues of cyt *c* and positive patch of cyt *f* and the hemes are shown in thick lines. Possible aspartic acid peptide binding sites of cyt *c* and cyt *f* are shown in solid arrows.

* To whom correspondence should be addressed.
† Graduate School of Science, Nagoya University.
‡ Meijo University.
§ Ibaraki University.
|| Research Center for Materials Science, Nagoya University.

(1) Hirota, S.; Endo, M.; Maeno, C.; Hibino, T.; Takabe, T.; Yamauchi, O. *J. Inorg. Biochem.* **1997**, *67*, 402.
(2) Hirota, S.; Hayamizu, K.; Endo, M.; Hibino, T.; Takabe, T.; Kohzuma, T.; Yamauchi, O. *J. Am. Chem. Soc.* **1998**, *120*, 8177−8183.
(3) Hirota, S.; Endo, M.; Tsukazaki, T.; Takabe, T.; Yamauchi, O. *J. Biol. Inorg. Chem.* **1998**, *3*, 563−569.

10.1021/ja9828455 CCC: $18.00
Published on Web 01/14/1999

Cyt *c* is a heme protein, positively charged at neutral pH, and functions as an electron-transporting protein by shuttling electrons from cytochrome c_1 in the bc_1 complex to the Cu_A site in cytochrome *c* oxidase (CcO). Cyt *c* also provides electrons to cytochrome *c* peroxidase (CcP) for the catalytic reduction of hydrogen peroxide. Crystal[4−8] and solution NMR[9,10] structures of cyt *c* showed charged amino acids distributed around the heme edge of cyt *c*, and it is suggested that an electrostatic interaction occurs between the positively charged residues of cyt *c* and the negatively charged residues of its reaction partners. X-ray crystallographic structures of horse cyt *c*−CcP and yeast iso-1 cyt *c*−CcP complexes showed that the basic sites of cyt *c* interact with the acidic sites of CcP.[11] The CcP-binding domain on the surface of horse cyt *c* was nearly identical to that defined by using derivatives of horse cyt *c* modified at individual Lys residues.[12] Site-directed mutagenesis studies have also been utilized for elucidating the cyt *c*−CcP binding interaction,[13,14] and it has recently been shown that this interaction can be modulated by groups which do not interact directly and may lie outside the interface defined by crystallographic studies.[15] The CcO recognition site of cyt *c* is also suggested to be mostly the exposed heme edge by chemical modification[16−18] and comparative kinetic studies of various cyt *c*.[19]

The cytochrome b_6f complex is an integral oligomeric membrane protein complex existing in the photosynthetic organism. Cyt *f* receives electrons from the Rieske iron−sulfur protein of the cytochrome b_6f complex and donates electrons to the soluble blue copper protein, plastocyanin (PC). X-ray crystallographic study of chloroplast cyt *f* revealed that a positive patch exists at its solvent-exposed site.[20] On the other hand, the crystal structures of plant oxidized and reduced PC's have been determined,[21−24] and two highly conserved sites have been considered as molecular recognition sites for its redox partners, cyt *f* and PSI: One site is located at the Cu-coordinating, solvent-accessible histidine (Cu-adjacent hydrophobic patch), and the other site is located at another solvent-accessible site containing acidic residues near a tyrosine residue (Cu-remote negative patch). The negative patch of PC has been indicated to be the cyt *f* interacting site through electrostatic interaction by recent studies,[25−33] whereas electron transfer from PC to P700 is suggested to follow through the hydrophobic patch.[34,35]

The constants for association between cyt *c* or cyt *f* and PC have been obtained by measuring the increase of the Soret band intensity of cyt *c* or cyt *f* on PC binding.[36−38] Recently cyt *f*/*c* and PC are proposed by Kostić et al. to bind and react with each other in different configurations, and computer simulation studies showed possible configurations for the diprotein complex formation.[39−41] A shift between the two conformations is required for the electron transfer, which is termed as the gating process.[42−46] Recent paramagnetic NMR and restrained rigid-body molecular mechanics studies by Ubbink et al. indicated that the electrostatic interactions guide PC and cyt *f* into a position that is optimal for electron transfer.[47] Conformational changes in cyt *c* upon noncovalent complex formations with CcO have been mentioned by various spectroscopic methods including resonance Raman spectroscopy.[48−53] Modification of

(4) Takano, T.; Trus, B. L.; Mandel, N.; Mandel, G.; Kallai, O. B.; Swanson, R.; Dickerson, R. E. *J. Biol. Chem.* **1977**, *252*, 776−785.
(5) Takano, T.; Dickerson, R. E. *J. Mol Biol.* **1981**, *153*, 79−94.
(6) Ochi, H.; Hata, Y.; Tanaka, N.; Kakudo, M.; Sakurai, T.; Aihara, S.; Morita, Y. *J. Mol. Biol.* **1983**, *166*, 407−418.
(7) Louie, G. V.; Brayer, G. D. *J. Mol. Biol.* **1990**, *214*, 527−555.
(8) Bushnell, G. W.; Louie, G. V.; Brayer, G. D. *J. Mol. Biol.* **1990**, *214*, 585−595.
(9) Banci, L.; Bertini, I.; Bern, K. L.; Gray, H. B.; Sompornpisut, P.; Turano, P. *Biochemistry* **1997**, *36*, 8992−9001.
(10) Banci, L.; Bertini, I.; Gray, H. B.; Luchinat, C.; Reddig, T.; Rosato, A.; Turano, P. *Biochemistry* **1997**, *36*, 9867−9877.
(11) Pelletier, H.; Kraut, J. *Science* **1992**, *258*, 1748−1755.
(12) Kang, C. H.; Brautigan, D. L.; Osheroff, N.; Margoliash, E. *J. Biol. Chem.* **1978**, *253*, 6502−6510.
(13) Erman, J. E.; Kresheck, G. C.; Vitello, L. B.; Miller, M. A. *Biochemistry* **1997**, *36*, 4054−4960.
(14) Miller, M. A.; Geren, L.; Han, G. W.; Saunders: A.; Beasley, J.; Pielak, G. J.; Durham, B.; Millet, F.; Kraut, J. *Biochemistry* **1996**, *35*, 667−673.
(15) Hake, R.; Corin, A.; McLendon, G. *J. Am. Chem. Soc.* **1997**, *119*, 10557−10558.
(16) Smith, H. T.; Staudenmayer, N.; Millett, F. *Biochemistry* **1977**, *16*, 4971−4974.
(17) Ferguson-Miller, S.; Brautigan, D. L.; Margoliash, E. *J. Biol. Chem.* **1978**, *253*, 149−159.
(18) Rieder, R.; Bosshard, H. R. *J. Biol. Chem.* **1978**, *253*, 6045−6053.
(19) Errede, B.; Kamen, M. D. *Biochemistry* **1978**, *17*, 1015−1027.
(20) Martinez, S. E.; Huang, D.; Szczepaniak, A.; Cramer, W. A.; Smith, J. L. *Structure* **1994**, *2*, 95−105.
(21) Guss, J. M.; Freeman, H. C. *J. Mol. Biol.* **1983**, *169*, 521−563.
(22) Colman, P. M.; Freeman, H. C.; Guss, J. M.; Murata, M.; Norris, V. A.; Ramshaw, J. A. M.; Venkatappa, M. P. *Nature* **1978**, *272*, 319−324.
(23) Guss, J. M.; Harrowell, P. R.; Murata, M.; Norris, V. A.; Freeman, H. C. *J. Mol. Biol.* **1986**, *192*, 361−387.
(24) Freeman, H. C. In *Coordination Chemistry-21*; Laurent, J. L., Ed.; Pergamon Press: Oxford, U.K., 1981; Vol. 21, pp 29−51.
(25) Takenaka, K.; Takabe, T. *J. Biochem.* **1984**, *96*, 1813−1821.
(26) Lee, B. H.; Hibino, T.; Takabe, T.; Weisbeek, P. J.; Takabe, T. *J. Biochem.* **1995**, *117*, 1209−1217.
(27) Meyer, T. E.; Zhao, Z. G.; Cusanovich, M. A.; Tollin, G. *Biochemistry* **1993**, *32*, 4552−4559.
(28) Adam, Z.; Malkin, R. *Biochim. Biophys. Acta* **1989**, *975*, 158−163.
(29) Morand, L. Z.; Frame, M. K.; Colvert, K. K.; Johnson, D. A.; Krogmann, D. W.; Davis, D. J. *Biochemistry* **1989**, *28*, 8039−8047.
(30) Gross, E. L.; Curtiss, A. *Biochim. Biophys. Acta* **1991**, *1056*, 166−172.
(31) Qin, L.; Kostić, N. M. *Biochemistry* **1992**, *31*, 5145−5150.
(32) Takabe, T.; Ishikawa, H.; Niwa, S.; Tanaka, Y. *J. Biochem.* **1984**, *96*, 385−393.
(33) Chapman, S. K.; Knox, C. V.; Sykes, A. G. *J. Chem. Soc., Dalton Trans.* **1984**, 2775−2780.
(34) Nordling, M.; Sigfridsson, K.; Young, S.; Lundberg, L. G.; Hansson, Ö. *FEBS Lett.* **1991**, *291*, 327−330.
(35) Haehnel, W.; Jansen, T.; Gause, K.; Klösgen, R. B.; Stahl, B.; Michl, D.; Huvermann, B.; Karas, M.; Herrmann, R. G. *EMBO J.* **1994**, *13*, 1028−1038.
(36) Modi, S.; Nordling, M.; Lundberg, L. G.; Hansson, Ö.; Bendall, D. S. *Biochim. Biophys. Acta* **1992**, *1102*, 85−90.
(37) He, S.; Modi, S.; Bendall, D. S.; Gray, J. C. *EMBO J.* **1991**, *10*, 4011−4016.
(38) Modi, S.; He, S.; Gray, J. C.; Bendall, D. S. *Biochim. Biophys. Acta* **1992**, *1101*, 64−68.
(39) Roberts, V. A.; Freeman, H. C.; Olson, A. J.; Tainer, J. A.; Getzoff, E. D. *J. Biol. Chem.* **1991**, *266*, 13431−13441.
(40) Ullmann, G. M.; Knapp, E.-W.; Kostić, N. M. *J. Am. Chem. Soc.* **1997**, *119*, 42−52.
(41) Ullmann, G. M.; Kostić, N. M. *J. Am. Chem. Soc.* **1995**, *117*, 4766−4774.
(42) Qin, L.; Kostić, N. M. *Biochemistry* **1993**, *32*, 6073−6080.
(43) Crnogorac, M. M.; Shen, C.; Young, S.; Hansson, Ö.; Kostić, N. M. *Biochemistry* **1996**, *35*, 16465−16474.
(44) Ivković-Jensen, M. M.; Kostić, N. M. *Biochemistry* **1996**, *35*, 15095−15106.
(45) Ivković-Jensen, M. M.; Kostić, N. M. *Biochemistry* **1997**, *36*, 8135−8144.
(46) Ivković-Jensen, M. M.; Ullmann, G. M.; Young, S.; Hansson, Ö.; Crnogorac, M. M.; Ejdebäck, M.; Kostić, N. M. *Biochemistry* **1998**, *37*, 9557−9569.
(47) Ubbink, M.; Ejdebäck, M.; Karsson, B. G.; Bendall, D. S. *Structure* **1998**, *6*, 323−335.
(48) Falk, K.-E.; Ångström, J. *Biochim. Biophys. Acta* **1983**, *722*, 291−296.
(49) Weber, C.; Michel, B.; Bosshard, H. R. *Proc. Natl. Acad. Sci. U.S.A.* **1987**, *84*, 6687−6691.
(50) Michel, B.; Bosshard, H. R. *Biochemistry* **1989**, *28*, 244−252.
(51) Michel, B.; Proudfoot, A. E. I.; Wallace, C. J. A.; Bosshard, H. R. *Biochemistry* **1989**, *28*, 456−462.
(52) Hildebrandt, P.; Heimburg, T.; Marsh, D.; Powell, G. L. *Biochemistry* **1990**, *29*, 1661−1668.

the structural and redox properties of cyt *c* upon binding to negatively charged heteropolytungstate, phospholipid vesicles, and silver electrodes has been reported.[54−58] To gain more detailed insights into the molecular recognition characters and the structural changes of cyt *c* and cyt *f* upon complex formation and their influence on structure−function relationship, we investigated the interaction of cyt *c* or cyt *f* with Aspptd's and the effects of Aspptd's and Lysptd's on the cyt *f*/*c*−PC electron transfer.

Experimental Section

Preparation of Samples. Bovine heart cyt *c*, Aspptd's (=Asp, *di*-Asp, *tri*-Asp, *tetra*-Asp, and *penta*-Asp) (Asp = aspartic acid), Lysptd's (=*tetra*-Lys and *penta*-Lys) (Lys = lysine), and *tetra*-Gly (Gly = glycine) were purchased from Sigma. Purification of oxidized and reduced cyt *c* were performed with a CM52 column (Whatman) after oxidizing or reducing it by adding a small amount of potassium ferricyanide or ascorbic acid solutions. *Brassica komatsuna* cyt *f* was purified according to a published method.[59] *Silene pratensis* (white campion) PC was expressed in *Escherichia coli* and purified by published methods.[26,60] Oligopeptides were first dissolved in 10 mM Tris-HCl buffer, pH 7.3 (or 7.4), with the peptide concentration of 40 mM, and then the pH value and the peptide concentration were readjusted to 7.3 (or 7.4) and 10 mM, respectively, by using 10 mM Tris-HCl buffer, pH 7.3 (or 7.4), and 0.1 N NaOH dissolved in 10 mM Tris. Concentrations of cyt *c*, cyt *f*, and PC were adjusted by their absorption spectra.

Optical Absorption Measurements. Optical absorption spectra were measured with a 2 mm-path length quartz cell at 15 °C on a Shimadzu UV 3101PC spectrophotometer.

Resonance Raman Measurements. Resonance Raman (RR) scattering was excited at 406.7 nm with a Kr^+ ion laser (Spectra Physics, 2060) and detected with a CCD (Astromed CCD, 3200) attached to a single polychromator (Ritsu Oyo Kogaku, DG-1000). The slit width and slit height were set to be 200 μm and 10 mm, respectively. The excitation laser beam power (at the sample point) was adjusted to 10 mW. Measurements were carried out at room temperature with a spinning cell (3000 rpm). The data accumulation time was 150 s. Raman shifts were calibrated with acetone, and the accuracy of the peak positions of the Raman bands was ± 1 cm^{-1}. The peptide concentration was chosen in such a way that a considerable change in the absorbance spectrum was caused without disturbing the Raman spectrum significantly by fluorescence.

Electrochemical Measurements. Cyclic voltammetry of cyt *f* and cyt *c* were carried out with a scan rate of 15 mV/s at room temperature using a voltammetric analyzer (Bioanalytical Systems, 100B). A 4,4′-dithiodipyridine-modified gold electrode was used as a working electrode, and a gold wire and an Ag/AgCl electrode were used as counter and reference electrodes, respectively.[61] The midpoint redox potentials were calibrated by using the redox poteinal of $[Co(phen)_3]^{2+/3+}$.[62] The concentrations of cyt *c* and cyt *f* were adjusted to 100 and 43 μM, respectively.

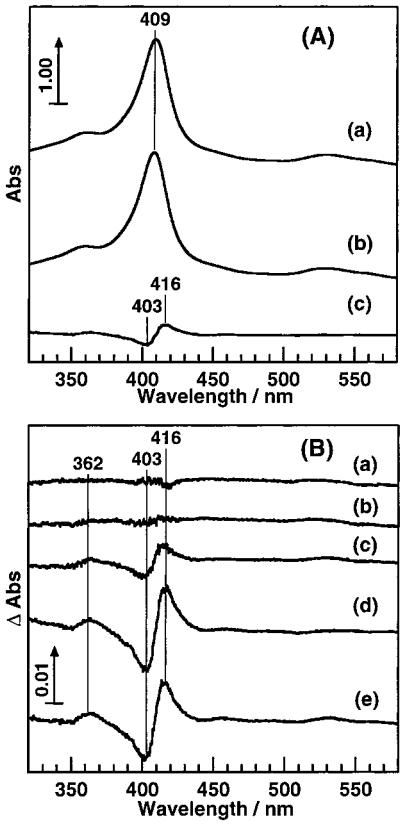

Figure 2. (A) Absorption spectra of oxidized cyt *c* (100 μM) (a) with and (b) without *tetra*-Asp (1 mM) and (c) their difference spectrum, spectrum a − spectrum b, multiplied by 30. (B) Difference absorption spectra between cyt *c* with and without various length of Aspptd's: (a) Asp, (b) *di*-Asp, (c) *tri*-Asp, (d) *tetra*-Asp, and (e) *penta*-Asp, respectively. The concentration of the Asp residues was adjusted to be the same between different length of Aspptd's: (a) Asp, 4 mM; (b) *di*-Asp, 2 mM; (c) *tri*-Asp, 1.3 mM; (d) *tetra*-Asp, 1 mM; (e) *penta*-Asp, 800 μM. Cell path length was 2 mm. Tris-HCl buffer (10 mM), pH 7.3, was used.

Kinetic Measurements. The electron-transfer rate constants from reduced cyt *c* or cyt *f* to oxidized PC in the presence of Aspptd's and Lysptd's were obtained by monitoring the absorbance at 420 and 422 nm, respectively, with an Otsuka Denshi RA601 stopped-flow equipment attached to a digital oscilloscope. For the cyt *c*−PC electron-transfer reaction, a 1 μM solution of cyt *c* in 10 mM Tris-HCl buffer, pH 7.3, containing 10 mM NaCl was mixed with 10 μM of PC in the same buffer solution. To investigate the inhibitory effect on the electron-transfer rate by charged peptides, we added Aspptd (0−600 μM) to the cyt *c* solution, the final peptide concentration being 0−300 μM after mixing cyt *c* and PC solutions. For the cyt *f*−PC system, a 1 μM solution of cyt *f* in 10 mM Tris-HCl buffer, pH 7.3, containing 60 mM NaCl was mixed with 10 μM of PC in the same buffer. The inhibitory effect of charged peptides on the electron-transfer rate was studied with a cyt *f* solution containing Aspptd (0−640 μM) or a PC solution containing Lysptd (0−640 μM), the peptide concentration being 0−320 μM after mixing cyt *f* and PC solutions. All the kinetic measurements were performed at 15 °C. Although the rate constants were very sensitive to the experimental conditions, especially the buffer and salt concentrations, the relative rate values were reproducible.

Results

Optical Absorption Measurements. The absorption spectra of oxidized cyt *c* (100 μM) with and without *tetra*-Asp (1 mM) and their difference spectrum (spectrum a − spectrum b) multiplied by 30 are shown in Figure 2A, which demonstrates the absorption change of cyt *c* upon interaction with *tetra*-Asp. A peak at 416 nm and a trough at 403 nm were detected near

(53) Hildebrandt, P.; Vanhecke, F.; Buse, G.; Soulimane, T.; Mauk, A. G. *Biochemistry* **1993**, *32*, 10912−10922.
(54) Chottard, G.; Michelon, M.; Herve, M.; Herve, G. *Biochim. Biophys. Acta* **1987**, *916*, 402−410.
(55) Hildebrandt, P. *Biochim. Biophys. Acta* **1990**, *1040*, 175−186.
(56) Hildebrandt, P.; Stockburger, M. *Biochemistry* **1989**, *28*, 6722−6728.
(57) Hildebrandt, P.; Heimburg, T.; Marsh, D. *Eur. Biophys. J.* **1990**, *18*, 193−201.
(58) Hildebrandt, P.; Stockburger, M. *Biochemistry* **1989**, *28*, 6710−6721.
(59) Matsuzaki, E.; Kamimura, Y.; Yamasaki, T.; Yakushiji, E. *Plant Cell Physiol.* **1975**, *16*, 237−246.
(60) Hibino, T.; Lee, B. H.; Takabe, T. *J. Biochem.* **1994**, *116*, 826−832.
(61) (a) Armstrong, F. A.; Hill, H. A. O.; Walton, N. J. *Acc. Chem. Res.* **1988**, *21*, 407−413. (b) Taniguchi, I.; Toyosawa, K.; Yamaguchi, H.; Yasuokouchi, K. *J. Chem. Soc., Chem. Commun.* **1982**, 1032−1033.
(62) Sykes, A. G. *Struct. Bonding* **1991**, *75*, 175−224.

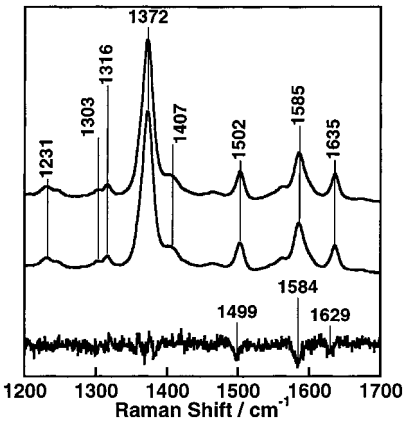

Figure 3. RR spectra in the 1200−1700 cm^{-1} region for (a) cyt *c* (50 μM) with *penta*-Asp (500 μM) and (b) cyt *c* without it and (c) their difference spectrum, spectrum a − spectrum b, multiplied by 15. The ordinate scales in spectra a and b are normalized with the intensity of the 1372 cm^{-1} band. Experimental conditions: slit width, 200 μm; slight height, 10 mm; excitation wavelength, 406.7 nm; laser power, 10 mW (at the sample point). Tris-HCl buffer (10 mM), pH 7.4, was used.

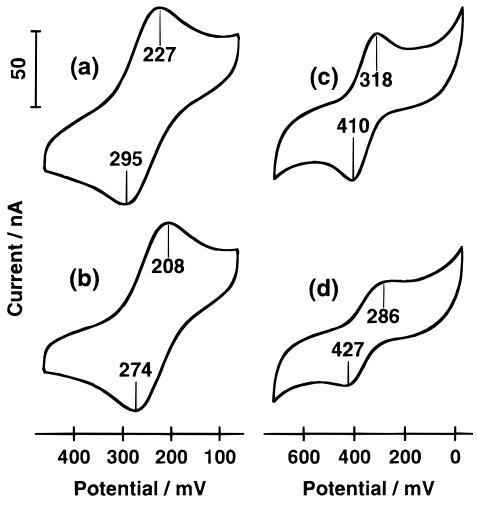

Figure 4. Cyclic voltammograms of cyt *c* (100 μM) and cyt *f* (43 μM) without and with *tetra*-Asp (3 mM). (a) cyt *c* without *tetra*-Asp, (b) cyt *c* with *tetra*-Asp, (c) cyt *f* without *tetra*-Asp, and (d) cyt *f* with *tetra*-Asp. Tris-HCl buffer (10 mM), pH 7.3, was used.

the Soret maximum of oxidized cyt *c* together with an additional peak at around 360 nm in the difference absorption spectrum. The wavelengths of these peaks were shifted from the Soret maximum of oxidized cyt *c* (409 nm). The cyt *c*−Aspptd interaction caused the Soret band at 409 nm of oxidized cyt *c* to shift to a little longer wavelength together with an increase of the absorption intensity at around 360 nm. The intensities of the peaks and trough increased as the concentration of Aspptd increased (data not shown). On the other hand, the intrinsic absorption change for cyt *f* on Aspptd interaction was not detectable, because slight reduction of cyt *f* occurred during the measurement, which might be due to the higher redox potential of cyt *f* compared to that of cyt *c* (see text below).

The difference absorption spectra between cyt *c* with and without Aspptd's of various length are shown in Figure 2B, where the concentrations of the Asp residues were adjusted to be the same among different Aspptd's. The difference peaks were also detected even for lower concentrations of *tri*-, *tetra*-, and *penta*-Asp, half of those used in Figure 2B, while no significant peak was detected when *di*-Asp, Asp, or *tetra*-Gly was used (data not shown).

Resonance Raman Measurements. Figure 3 exhibits the RR spectra in the 1200−1700 cm^{-1} region for cyt *c* (50 μM) with and without *penta*-Asp (500 μM) excited at 406.7 nm and their difference spectrum (spectrum a − spectrum b) multiplied by 15, where troughs were detected at 1499, 1584, and 1629 cm^{-1}. No significant peak was detected when *tetra*-Gly was used instead of *penta*-Asp or when the concentration of Tris was raised from 10 to 50 mM (data not shown). The difference spectrum c shows that the RR spectrum of cyt *c* is perturbed on complex formation with *penta*-Asp, which indicates that structural changes occur at the heme site of cyt *c* due to complex formation. The spectral change of spectrum c showed similar changes which were detected for the RR spectrum of cyt *c* on complex formation with CcO, where negative features were detected with minima at ∼1495 and 1635−1640 cm^{-1}.[53]

Electrochemical Measurements. Figure 4 depicts the cyclic voltammograms obtained for cyt *c* (100 μM) and cyt *f* (43 μM) without and with *tetra*-Asp (3 mM), all of which showed well-defined quasi-reversible faradaic responses. In the absence of Aspptd the midpoint potentials ($E_{1/2}$) of cyt *c* and cyt *f* were in good agreement with the reported values.[31,63,64] However, they shifted to lower poteintals by about 7−20 mV upon addition of *tetra*-Asp. $E_{1/2}$ of cyt *c* shifted to a lower potential as the concentration of Aspptd increased, and the shift was relatively sensitive to the *tetra*-Asp concentration when it was < 1 mM and less sensitive to that when it was > 1 mM (Table 1).

Kinetic Measurements. To investigate the nature of the interactions between Aspptd's and cyt *c* or cyt *f* in more detail, we performed stopped-flow measurements on the electron transfer between reduced cyt *c* and oxidized PC in the presence of Aspptd's (Figure 5) and compared the results obtained for addition of Lysptd's in the same system.[2] We also performed measurements on the electron transfer between reduced cyt *f* and oxidized PC in the presence of Aspptd's or Lysptd's (Figure 6). The electron-transfer rate became slower in the presence of Aspptd's or Lysptd's for both systems. The electron transfer was not affected when the same amount of *tetra*-Gly was added (data not shown), showing that the effect of the peptide terminal charges of the $-COO^-$ and $-NH_3^+$ groups can be neglected. Inhibition of the electron transfer was not prominent when shorter peptides (tri, di, or mono) were used, due to their weaker electrostatic interactions with the proteins. These inhibitory effects are therefore due to the competitive inhibition by electrostatic interactions of cyt *c* or cyt *f* with Aspptd's and of PC with Lysptd's. The inverse plots of the observed electron-transfer rate constants (k_{obs}) versus the initial concentrations of Lysptd's in the cyt *c*−PC system and Aspptd's and Lysptd's in the cyt *f*−PC system gave a straight line (Figure 6 and Figure 5 of ref 2), while higher concentrations of Aspptd's were required for effective electron-transfer inhibition in the cyt *c*−PC system (Figure 5). The difference in the inhibition character could be attributed to the difference in the structural features of cyt *c* and cyt *f*; the positive charges are spread out around the exposed heme edge for cyt *c* whereas cyt *f* possesses a positive patch (Figure 1).

Discussion

Aspptd's Binding to Cyt *c* and Its Effect on Protein Structure. The electron-transfer rate constant between reduced

(63) Harris, D.; Johnson, A. W. *J. Chem. Soc. Chem. Commun.* **1977**, 771−772.
(64) Salamon, Z.; Hazzard, J. T.; Tollin, G. *Proc. Natl. Acad. Aci. U.S.A.* **1993**, *90*, 6420−6423.

Table 1. Midpoint Redox Potentials ($E_{1/2}$) of Cyt *c* (100 μM) in the Presence of Different Concentrations of *tetra*-Asp (vs NHE)[a]

tetra-Asp/μM	0	100	300	500	700	1000	1500	2000	2500	3000
$E_{1/2}$/mV	261	261	255	252	251	250	247	246	246	241

[a] In 10 mM phosphate buffer, pH 7.3, at 15 °C. [b] Accuracy of $E_{1/2}$ is 3 mV.

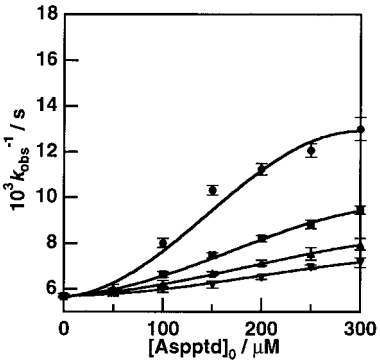

Figure 5. Plots of the reciprocal electron-transfer rate constants ($1/k_{obs}$) for the reduced cyt *c*−oxidized PC system vs the initial concentrations of Aspptd's: ▼ = *di*-, ▲ = *tri*-, ■ = *tetra*-, and ● = *penta*-Asp. Experimental conditions: sample concentrations, cyt *c*, 0.5 μM, PC, 5 μM; 15 °C. Tris-HCl buffer (10 mM), pH 7.3, containing 10 mM NaCl was used.

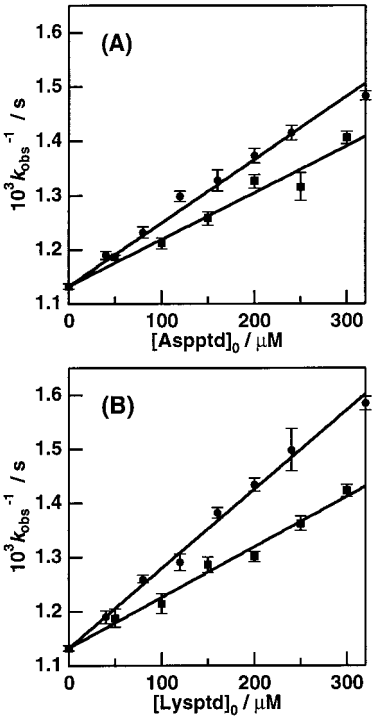

Figure 6. Plots of the reciprocal electron-transfer rate constants ($1/k_{obs}$) for the reduced cyt *f*−oxidized PC system vs the initial concentrations of charged peptides together with least-squares fitted lines according to eq 3: (A) Aspptd's and (B) Lysptd's, ■ = tetra- and ● = pentapeptides. Experimental conditions: sample concentrations, cyt *f*, 0.5 μM, PC, 5 μM; 15 °C. Tris-HCl buffer (10 mM), pH 7.3, containing 60 mM NaCl was used.

cyt *c* or cyt *f* and oxidized PC decreased in the presence of Aspptd's or Lysptd's, suggesting that Aspptd's and Lysptd's could interact with the proteins and inhibit the electron transfer. Similar inhibitory effects by Lysptd's in the cyt *c*−PC electron transfer have been detected, which have been explained by the electrostatic interaction between PC and Lysptd's.[1,2]

Since Aspptd's do not have any absorption band in the visible region, changes in the spectrum of cyt *c* due to the interaction with Aspptd's can be investigated in detail, and they were detected for *tri*-, *tetra*-, and *penta*-Asp (Figure 2B), while they were missing for *di*-Asp and Asp. This dependence on the length of Aspptd's is in line with the kinetic results, suggesting that electrostatic interactions with *tri*-, *tetra*-, or *penta*-Asp are strong enough to make electrostatic complexes, while those with *di*-Asp or Asp are not. The increase in the absorption spectral changes with *tetra*-Asp concentration supports that the changes are due to complex formation between cyt *c* and *tetra*-Asp. The extent of the changes decreased significantly when the same amounts of *tetra*-Gly, *tetra*-Lys, or NaCl instead of *tetra*-Asp were used (data not shown), which also supports that the formation of cyt *c*−Aspptd complexes are due to electrostatic interactions. The results further indicate that the cyt *c* heme geometry is perturbed when cyt *c* interacts with Aspptd's. However, it was not possible to obtain binding constants for peptide binding to cyt *c*, since the changes did not reflect a simple complex formation character probably due to existence of a number of peptide interacting sites in cyt *c*.

The difference absorption spectrum, the spectrum of oxidized cyt *c* in the presence of oxidized PC *minus* the respective spectra of oxidized cyt *c* and oxidized PC, showed a difference pattern at 416−403 nm and a peak at 362 nm (data not shown). The difference spectra between cyt *c* with and without Aspptd's and PC showed a similar difference pattern (416−403 nm) with a peak at 362 nm, which indicates that Aspptd's perturb the geometry of cyt *c* in the same way as PC does and that cyt *c* exhibits a similar conformational change on interaction with Aspptd's and PC. Therefore, we infer that Aspptd's could be used as models for the cyt *c* interacting sites of proteins.

Troughs were detected at 1499, 1584, and 1629 cm^{-1} in the difference RR spectrum between cyt *c* (50 μM) with and without *penta*-Asp (500 μM). The RR spectrum of the heme of cyt *c* has been assigned precisely,[65] and the troughs at 1499, 1584, and 1629 cm^{-1} might be caused by the changes of the ν_3 (1502 cm^{-1}), ν_2 (1585 cm^{-1}), and ν_{10} (1635 cm^{-1}) bands, respectively, whose frequencies are sensitive to the oxidation, coordination, and spin state of the heme iron.[66,67] The observed RR spectral changes indicate that the heme conformation is perturbed upon Aspptd binding to cyt *c*. Hildebrandt et al. reported similar spectral changes for the ν_3 and ν_{10} bands of cyt *c* upon binding with CcO[53] and explained them as due to formation of a more open heme pocket structure termed as conformational state II. The heme iron in this state is shown to exist in a mixture of five-coordinated high-spin and six-coordinated low-spin configurations by absorbing cyt *c* on a silver electrode.[58] The similarity of the cyt *c* RR spectral changes upon Aspptd and CcO binding to cyt *c* supports the absorption spectral results that Aspptd interacts with cyt *c* in the same way as CcO.

Cyt *c* and Cyt *f* Redox Potential Changes due to Interactions with Aspptd's. The $E_{1/2}$ of cyt *c* and cyt *f* shifted to lower potentials by adding *tetra*-Asp to their solution (Figure 4), and the potentials of cyt *c* and cyt *f* shifted lower by about 7−20 mV upon addition of 3 mM *tetra*-Asp. The $E_{1/2}$ of cyt *c* shifted

(65) Hu, S.; Morris, I. K.; Singh, J. P.; Smith, K. M.; Spiro, T. G. *J. Am. Chem. Soc.* **1993**, *115*, 12446−12458.
(66) Spiro, T. G.; Burke, J. M. *J. Am. Chem. Soc.* **1976**, *98*, 5482−5489.
(67) Parthasarathi, N.; Hansen, C.; Yamaguchi, S.; Spiro, T. G. *J. Am. Chem. Soc.* **1987**, *109*, 3865−3871.

to a lower potential as the concentration of *tetra*-Asp increased, and the potential shift was prominent for *tetra*-Asp concentrations at < 1 mM and small at > 1 mM, which suggests that the negative shift in its redox potential is due to the cyt *c*−*tetra*-Asp interaction. Therefore, we infer that the above-mentioned structural change of cyt *c* due to interactions with Aspptd's shifts its redox potential to a lower potential and makes it easier to provide an electron to its redox partners. The detected structural change due to interaction with Aspptd's might be similar to that suggested by NMR studies[68] and might cause a negative shift in its redox potential. A negative shift for the redox potential of cyt *c* absorbed on a silver electrode by changing the electrode potential has been reported, which shift was suggested due to the opening of the heme crevice or modified hydrogen-bonding interaction of the heme propionates.[58] The $E_{1/2}$ negative shift observed for cyt *c* upon Aspptd binding might be due to the same conformational changes observed for cyt *c* absorbed on a silver electrode.

The $E_{1/2}$ of silene PC and *Brassica komatsuna* cyt *f* are 343[2] and 364 mV, respectively, when no charged peptides are added to their solutions (Figure 4). By consideration of only these $E_{1/2}$ values, the electron transfer would not occur between these protein. However, we previously showed that the $E_{1/2}$ of PC shifts to a higher potential by its conformational change on interaction with Lysptd's at its PC negative patch.[2] In this study, the $E_{1/2}$ of cyt *f* shifted to a lower potential on interaction with *tetra*-Asp. These $E_{1/2}$ changes taken together, suggest that cyt *f* and PC would suffer conformational changes on complex formation to facilitate the electron transfer between them.

Kinetic Consideration on Aspptd's Binding to Cyt *c* and Cyt *f*. It is of fundamental importance to know how proteins recognize their electron-accepting and/or -donating partners. Electron transfers between cyt *c* or cyt *f* and PC have been studied extensively,[26−31,36,44−46,69,70] and small inorganic compounds have been shown to inhibit the electron transfer between cyt *c* or cyt *f* and PC.[33,71−74] In our previous studies, the electron-transfer rate from cyt *c* to PC became slower in the presence of Lysptd's.[1,2] We attributed this effect to formation of competitive inhibitors by electrostatic interactions between PC and Lysptd's.[1,2] In this study, the electron transfer from reduced cyt *c* or cyt *f* to oxidized PC became slower in the presence of Aspptd's or Lysptd's, and the inhibitory effect became prominent for longer (penta > tetra > tri > di > mono) peptides and at higher concentrations of peptides.

The observed inhibition by Aspptd's and Lysptd's in the cyt *f*−PC system may be interpreted in the same way as we previously did for that observed for Lysptd's in the cyt *c*−PC system by considering formation of two complexes:[1,2] a cyt *f*−PC complex, where electron transfer occurs subsequently, and a cyt *f*−Aspptd or PC−Lysptd complex, which competitively inhibit the formation of the cyt *f*−PC complex and thus the electron transfer. We assumed that Lysptd binds only at the PC negative patch effectively, since it is well established experimentally that the negative patch of PC is the cyt *c* or cyt *f* interaction site.[25−33] Moreover, the electron-transfer rate from reduced cyt *c* to oxidized PC and the inhibitory effects of Lysptd's decreased upon decreasing the net charge of the PC negative patch by mutation, which strongly supports that the negative patch is the dominant cyt *c* recognition site.[1,2] The complex formations are expressed by the following equations:

$$\text{cyt } f_{red} + \text{Aspptd} \overset{K_i}{\rightleftharpoons} (\text{cyt } f_{red}\cdot\text{Aspptd}) \quad (1A)$$

$$\text{PC}_{ox} + \text{Lysptd} \overset{K_i'}{\rightleftharpoons} (\text{PC}_{ox}\cdot\text{Lysptd}) \quad (1B)$$

$$\text{cyt } f_{red} + \text{PC}_{ox} \overset{K_{OS}}{\rightleftharpoons} (\text{cyt } f_{red}\cdot\text{PC}_{ox}) \xrightarrow{k_e} (\text{cyt } f_{ox}\cdot\text{PC}_{red}) \quad (2)$$

were K_i, K_i', and K_{OS} are the association constants for cyt f_{red}−Aspptd, PC_{ox}−Lysptd, and cyt f_{red}−PC_{ox} complexes, respectively, and k_e represents the electron-transfer rate constant.

The dissociation of cyt *f*−Aspptd or PC−Lysptd complexes to cyt *f* and Aspptd or to PC and Lysptd will not be the rate-limiting steps, because the observed electron-transfer rate was affected by the concentration of Aspptd's and Lysptd's. If we write the observed rate constant as k_{obs}, $K_{OS}k_e$ as k, and the initial concentrations of PC, Aspptd, and Lysptd as $[PC]_0$, $[Aspptd]_0$, and $[Lysptd]_0$, respectively, we obtain the following relationships:

$$\frac{1}{k_{obs}} = \frac{K_i}{k[PC]_0}[Aspptd]_0 + \frac{1}{k[PC]_0} \quad (3A)$$

$$\frac{1}{k_{obs}} = \frac{K_i'}{k[PC]_0}[Lysptd]_0 + \frac{1}{k[PC]_0} \quad (3B)$$

Plots of $1/k_{obs}$ vs $[Aspptd]_0$ and $[Lysptd]_0$ gave lines shown in Figure 6, substantiating the validity of the assumptions leading to eqs 3A,B. Table 2 summarizes the K_i and K_i' values obtained from the plots. Since the fitting assuming one peptide binding to each protein was successful, it is reasonable to assume that only one Aspptd is bound to cyt *f* and one Lysptd is bound to PC.

Since the inhibition by both Aspptd's and Lysptd's in the cyt *f*−PC system fitted well with the above-discussed equations (eqs 1−3), cyt *f* would recognize PC in the similar way as PC recognizes cyt *f* through its negative patch. This inhibitory character confirms the results suggested by X-ray crystallographic and computer simulation studies that cyt *f* has a positive patch with basic amino acid residues which interacts specifically with the negative patch of PC.[20,40,47,75] K_i and K_i' were larger for the pentapeptide compared to the tetrapeptide (Table 2), and the association constants obtained for cyt *f* and Aspptd's and for PC and Lysptd's with the same peptide length, showed similar values (cyt *f*−*tetra*-Asp and PC−*tetra*-Lys, cyt *f*−*penta*-Asp and PC−*penta*-Lys). Therefore, cyt *f* and PC would interact with Aspptd's and Lysptd's, respectively, with

Table 2. Association Constants (K_i and K_i') for Cyt *f*−Aspptd and PC−Lysptd Complexes[a]

length of peptide	association constant/M^{-1}	
	cyt *f*−Aspptd (K_i)	PC−Lysptd (K_i')
tetra	760 ± 60	820 ± 50
penta	1000 ± 100	1300 ± 100

[a] In 10 mM Tris-HCl buffer, pH 7.3, containing 60 mM NaCl, at 15 °C.

(68) Ubbink, M.; Bendall, D. S. *Biochemitstry* **1997**, *36*, 6326−6335.
(69) Anderson, G. P.; Sanderson, D. G.; Lee, C. H.; Durell, S.; Anderson, L. B.; Gross, E. L. *Biochim. Biophys. Acta* **1987**, *894*, 386-398.
(70) Soriano, G. M.; Ponamarev, M. V.; Tae, G.-S.; Cramer, W. A. *Biochemistry* **1996**, *35*, 14590−14598.
(71) McGinnis, J.; Sinclair-Day, J. D.; Sykes, A. G. *J. Chem. Soc., Dalton Trans.* **1986**, 2007−2009.
(72) Chapman, S. K.; Sanemasa, I.; Sykes, A. G. *J. Chem Soc., Dalton Trans.* **1983**, 2549−2553.
(73) Chapman, S. K.; Watson, A. D.; Sykes, A. G. *J. Chem. Soc., Dalton Trans.* **1983**, 2543−2548.
(74) Beoku-Betts, D.; Chapman, S. K.; Knox, C. V.; Sykes, A. G. *Inorg. Chem.* **1985**, *24*, 1677−1681.
(75) Pearson, D. C., Jr.; Gross, E. L. G.; David, E. S. *Biophys. J.* **1996**, *71*, 64−76.

similar electrostatic strength, and thus cyt *f* and PC would recognize each other almost equally.

For the cyt *c*−PC system, the inhibition by Lysptd's followed the equations obtained by the discussion above (eqs 1−3), while that by Aspptd's did not: The inhibitions by Aspptd's were not significant when the Aspptd's concentrations were low, and higher concentrations of Aspptd's were required for effective inhibition. The difference in the inhibitory character between Lysptd's and Aspptd's may be interpreted as due to the difference in the manner cyt *c* and PC recognize their reaction partners, since the distribution of the charged amino acids on the surface of each protein is different (Figure 1). An aforementioned NMR study on the cyt *c*−PC complex showed that the negative patch of PC is the interaction site with cyt *c*, while a large area around the heme edge of cyt *c* is involved in the interaction with PC.[68] From the inhibitory pattern shown in Figure 5, we infer that the inhibition by Aspptd could occur only when the positive charges around the heme edge are considerably blocked by Aspptd by formation of cyt *c*−Aspptd$_n$ ($n > 1$) complexes, which should require a certain concentration of Aspptd.

Conclusion

Absorption spectral studies of cyt *c* with various lengths of Aspptd's showed that cyt *c* interacts with Aspptd's by electrostatic interactions, and it interacts effectively only with Aspptd's equal to or longer than *tri*-Asp. Absorption spectral changes of cyt *c* were the same for cyt *c*−PC and cyt *c*−Aspptd's interactions, indicating that Aspptd's are good models for the cyt *c* recognition site of proteins. Resonance Raman studies also demonstrated the conformational changes at the heme site of cyt *c* on binding of Aspptd, which changes were similar to those observed for CcO binding.[53] Electrochemical studies showed that the redox potentials of cyt *c* and cyt *f* shift to lower potentials on interaction with Aspptd's, making cyt *c* and cyt *f* fit for providing an electron to their redox partners. The observed structural change of cyt *c* might be connected to the redox change, and the redox potentials of cyt *f* and PC shift to lower and higher potentials, respectively, upon complex formation with the Aspptd's and Lysptd's, respectively, which would indicate these redox changes facilitate its electron transfer.

The electron-transfer rate constant between reduced cyt *c* or cyt *f* and oxidized PC decreased in the presence of Aspptd's or Lysptd's. The inhibitory character by Aspptd's on the cyt *f*−PC electron transfer suggested that cyt *f* recognizes PC through a specific positive patch by electrostatic interactions. On the other hand, the inhibition of Aspptd's on the cyt *c*−PC system was not significant when the Aspptd concentration was low, and higher concentrations for effective inhibition were required. The difference in the inhibitory character between these systems may be interpreted as due to the difference in the manner cyt *c* and cyt *f* recognize PC. A special positive patch of cyt *f* is the interaction site with PC,[20,40,47,75] while a large area around the heme edge of cyt *c* is involved in the interaction with PC.[68]

Since Aspptd's do not have any absorption peaks in the visible spectral region, it was possible to detect the structural change of cyt *c* by following its absorption spectral changes. In addition, it will be possible to study the molecular recognition character of proteins in detail by systematically varying the length and charge of the peptides.

Acknowledgment. The authors thank Prof. Teizo Kitagawa, Institute for Molecular Science, for the use of the resonance Raman equipment. This work was supported by Grants-in-Aid for Scientific Research to O.Y. and S.H. (No. 09304062), for Encouragement of Young Scientists to S.H. (No. 10740304), and for Priority Areas (Metal-Assembled Complexes) to O.Y. (No. 10149219) and (Molecular Biometallics) to T.K. (No. 09235202) from the Ministry of Education, Science, Sports, and Culture of Japan. The Grant Aid of the Ground Experiment for the Space Utilization from the Japan Space Forumand National Space Developments Agency of Japan to T.K is also gratefully acknowledged.

JA9828455